JACS
JOURNAL OF THE AMERICAN CHEMICAL SOCIETY
Article
pubs.acs.org/JACS

UO_2^{2+} Uptake by Proteins: Understanding the Binding Features of the Super Uranyl Binding Protein and Design of a Protein with Higher Affinity

Samuel O. Odoh,*[,†] Gary D. Bondarevsky,[†] Jason Karpus,[‡] Qiang Cui,[§] Chuan He,[‡] Riccardo Spezia,[∥] and Laura Gagliardi*[,†]

[†]Department of Chemistry, Chemical Theory Center, and Supercomputing Institute, University of Minnesota, Minneapolis, Minnesota 55455-0431, United States

[‡]Department of Chemistry and Institute of Biophysical Dynamics, The University of Chicago, 929 East 57th Street, Chicago, Illinois 60637, United States

[§]Department of Chemistry, University of Wisconsin—Madison, 1101 University Avenue, Madison, Wisconsin 53706, United States

[∥]CNRS, Laboratoire Analyse et Modélisation pour la Biologie et l'Environnement, UMR 8587, Université d'Evry-Val-d'Essonne, 91025, Every Cedex, France

Supporting Information

ABSTRACT: The capture of uranyl, UO_2^{2+}, by a recently engineered protein (Zhou et al. *Nat. Chem.* **2014**, *6*, 236) with high selectivity and femtomolar sensitivity has been examined by a combination of density functional theory, molecular dynamics, and free-energy simulations. It was found that UO_2^{2+} is coordinated to five carboxylate oxygen atoms from four amino acid residues of the super uranyl binding protein (SUP). A network of hydrogen bonds between the amino acid residues coordinated to UO_2^{2+} and residues in its second coordination sphere also affects the protein's uranyl binding affinity. Free-energy simulations show how UO_2^{2+} capture is governed by the nature of the amino acid residues in the binding site, the integrity and strength of the second-sphere hydrogen bond network, and the number of water molecules in the first coordination sphere. Alteration of any of these three factors through mutations generally results in a reduction of the binding free energy of UO_2^{2+} to the aqueous protein as well as of the difference between the binding free energies of UO_2^{2+} and other ions (Ca^{2+}, Cu^{2+}, Mg^{2+}, and Zn^{2+}), a proxy for the protein's selectivity over these ions. The results of our free-energy simulations confirmed the previously reported experimental results and allowed us to discover a mutant of SUP, specifically the GLU64ASP mutant, that not only binds UO_2^{2+} more strongly than SUP but that is also more selective for UO_2^{2+} over other ions. The predictions from the computations were confirmed experimentally.

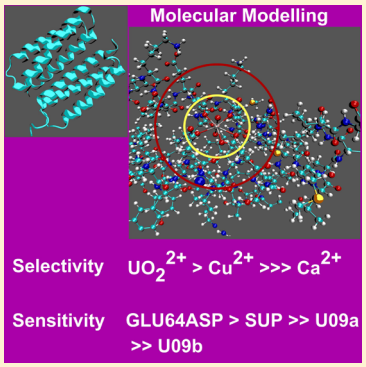

INTRODUCTION

The long-term goals of actinide chemistry research are the improvement of the separation and storage of radioactive materials as well as the development of more efficient approaches for remediating contaminated environments and decorporating mammalian tissues.[1,2] To this end, there are some macromolecules (proteins[3−9] and lipopolysaccharides[10−12]) that have significant potential for use in capturing the uranyl group, UO_2^{2+}, from contaminated environments and living tissues. This is important, as UO_2^{2+} is the dominant species for the most common oxidation state of uranium, +6. It is therefore of great interest that Zhou et al. have recently engineered a protein with femtomolar sensitivity for UO_2^{2+}.[13] This protein, labeled SUP (super uranyl binding protein: 4FZO[14] and 4FZP[15]), is thermally stable and exhibits in excess of 10000-fold selectivity for UO_2^{2+} over other cations. This degree of sensitivity and selectivity for UO_2^{2+} is a major breakthrough for its capture and sequestration from the environment as well as for treatment protocols for radionuclide poisoning. There are however some open questions regarding the origins of the exceptional sensitivity and selectivity of this protein for UO_2^{2+}. First, the exact binding mode of UO_2^{2+} to SUP in aqueous solutions and at neutral/alkaline pH values is not fully understood. SUP was crystallized under acidic conditions (pH of 4.5).[13] In the crystal structure, only the ASP68 and GLU17 residues of SUP directly bind UO_2^{2+}. In addition, UO_2^{2+} is also bound to a water ligand. It should however be noted that the coordination of UO_2^{2+} by SUP would be different under the aqueous neutral/alkaline conditions where the protein displays its exceptional selectivity and sensitivity.

Second, Zhou et al.[13] designed SUP by inducing several mutations in the 2PMR protein of *Methanobacterium*

Received: August 25, 2014
Published: November 19, 2014

 © 2014 American Chemical Society dx.doi.org/10.1021/ja5087563 | *J. Am. Chem. Soc.* 2014, 136, 17484−17494

thermoautotrophicum.[16] Some of these mutations are ASN13ASP, GLN64GLU, and LEU67THR. As 2PMR is significantly poorer than SUP in capturing UO_2^{2+}, these mutations are important to the sensitivity and selectivity of the latter. There is therefore a need to ascertain how the ASP13 and GLU64 residues exert their importance on UO_2^{2+} capture. This is all the more intriguing, as the crystal structure obtained at pH 4.5 indicates that UO_2^{2+} does not interact with ASP13 or GLU64. An adequate understanding of the effects of the ASN13ASP, GLN64GLU, and LEU67THR mutations on the selectivity and sensitivity of UO_2^{2+} capture can provide insights into potential mutations that can be used to engineer proteins that bind UO_2^{2+} more strongly than SUP and that are more selective for UO_2^{2+} over other ions.

In addition, the roles of the ARG71 and THR67 residues in UO_2^{2+} capture have to be elucidated.[13] Zhou et al.[13] found that proteins in which THR67 is replaced by LEU are about 30 times less sensitive toward UO_2^{2+}. The exact role of THR67 during UO_2^{2+} capture is however not fully understood. In the crystal structure,[13] ARG71 forms hydrogen bonds with the oxygen atoms of UO_2^{2+} and a salt bridge with GLU17. It was suggested that the hydrogen bonds to the oxygen atoms of UO_2^{2+} might also be responsible for the recognition of the vanadyl cation, VO^{2+}, in contrast to the lower binding of other cations such as Ca^{2+} and K^+.[13] This however does not explain why SUP is 3400 times more selective for UO_2^{2+} than Cu^{2+}, 9400 times more selective for UO_2^{2+} than VO^{2+}, and 10^5–10^8 times more selective for UO_2^{2+} than 15 other cations.[13]

In this work, we have used molecular dynamics (MD) and free-energy simulations to study the UO_2^{2+}–SUP protein system. The motivations for this study are 4-fold:

(a) **Coordination Environment:** We would like to determine the coordination environment of UO_2^{2+} in SUP under the aqueous conditions in which the protein displays its exceptional capture properties. This extends to the first shell around UO_2^{2+} as well to the ARG71 and THR67 residues with which it has no direct interaction. We are also interested in the mechanism by which THR67 exacts a tremendous effect on SUP's selectivity and sensitivity for UO_2^{2+}.

(b) **Mutation Effects and Sensitivity for UO_2^{2+}:** We would like to provide insights into the reasons why proteins with any combination of the ASN13ASP, GLN64GLU, and LEU67THR mutations displayed significantly poorer sensitivities for UO_2^{2+}.

(c) **Origins of UO_2^{2+} Selectivity:** We would like to determine the reasons why SUP is so strongly selective for UO_2^{2+}. As noted, the protein is also modestly selective for Cu^{2+} and VO^{2+} in contrast to other metal ions.

(d) **Search for Protein(s) with Higher UO_2^{2+} Binding Affinities:** An understanding of the UO_2^{2+} capture properties of SUP as well as the effects of the mutations employed during the experimental discovery of SUP was the basis for the design of a mutant with greater sensitivity and selectivity for UO_2^{2+} than SUP.

COMPUTATIONAL METHODOLOGY

Molecular Dynamics Simulations. *System Setup.* The simulation system consists of SUP and UO_2^{2+} solvated in a cubic box of water. The box extended 2.0 nm around the protein. The AMBER99sb-ildn force field[17] was used for the amino acid residues of the protein, while the surrounding water was described with the SPCE[18] model. Sodium ions were used to neutralize the charge of the whole system. The starting structure was initially quenched with a steepest descent algorithm for up to 5000 steps or until the maximum force is less than 1000 kJ/(mol·nm). The system was then equilibrated for 0.5 ns at 300 K (NVT ensemble) and subsequently for 2.0 ns at 300 K and 1 bar (NPT ensemble) while the coordinates of the protein and UO_2^{2+} were fixed. During the NPT equilibration steps, the isothermal compressibility of water was set at 4.5×10^{-5} bar^{-1} and the Parrinello–Rahman barostat[19] was used to maintain the pressure. The linear constraint solver (LINCS)[20] algorithm was used to constrain all bonds during these equilibration steps. A neighbor list cutoff of 1.2 nm was employed, and electrostatic interactions were calculated at every step with the particle-mesh Ewald (PME) method.[21] Short-range dispersion interactions were described by a Lennard-Jones potential with a cutoff of 1.2 nm. Long-range dispersion corrections for energy and pressure were applied. After equilibration, production simulations were carried out for 10–90 ns at 300 K with no constraints on UO_2^{2+} and the protein while employing the Nosé–Hoover thermostat.[22] In these simulations, we used the leapfrog integrator with a 2 fs integration time-step. The conformations of the whole system were stored every 2 ps.

Uranyl Parameters. The force field parameters used to describe UO_2^{2+} were taken from the work of Pomogaev et al.[23] This is a nonpolarizable flexible force field that performs quite well for the description of UO_2^{2+} in water[23] and in mixed water–ionic liquid solutions.[24,25] Lorentz–Berthelot mixing rules were used to combine this force field with the AMBER99sb-ildn[17] force field used for the protein. In aqueous solution, MD simulations with this force field predict that UO_2^{2+} coordinates five water molecules, in good agreement with previous experimental and computational reports.[26−31]

Free-Energy Simulations. The selectivity of SUP for UO_2^{2+} over other ions was described by the free energies needed to change a captured UO_2^{2+} group to Ca^{2+}, Cu^{2+}, Mg^{2+}, or Zn^{2+}. These are the differences between the binding energies of UO_2^{2+} and $Ca^{2+}/Cu^{2+}/Mg^{2+}/Zn^{2+}$ and were obtained with thermodynamic perturbation simulations.[32] A total of 11 windows (in steps of 0.1) were used to interpolate the initial state (λ = 1; UO_2^{2+}) and the final state (λ = 0; $Ca^{2+}/Cu^{2+}/Mg^{2+}/Zn^{2+}$). We first interpolated the electrostatic parameters before interpolating the van der Waals (vdW) parameters. This approach for changing UO_2^{2+} to other cations has been used by Guilbaud and Wipff on analogous systems.[33] Each window consists of a 250 ps equilibration period and a 1.3 ns sampling period.

In addition to these free-energy simulations, we performed several 90 ns simulations of Ca^{2+}, Cu^{2+}, Mg^{2+}, and Zn^{2+} bound to aqueous SUP at a similar binding site to that occupied by UO_2^{2+}. We examined the binding motifs of these ions to SUP using several independent trajectories. Two examples involve (a) simply replacing UO_2^{2+} bound to SUP by a transition metal ion and (b) adding an ion to different trajectories obtained from simulations of the SUP protein. For Ca^{2+}, Cu^{2+}, Mg^{2+}, and Zn^{2+}, we have used the force field parameters native to the AMBER99sb-ildn[17] set.

To describe the binding of UO_2^{2+} to SUP, similar free-energy simulations were carried out in which the electrostatic and vdW parameters of the captured UO_2^{2+} were switched off [λ = 1; UO_2^{2+} (charge and vdW parameters of uranium and oxygen

dx.doi.org/10.1021/ja5087563 | J. Am. Chem. Soc. 2014, 136, 17484−17494

Table 1. Proteins Studied in This Work

synthesized proteins[13]	intermediate proteins	potential proteins
SUP	ASP13ASN	ASP68GLU
U09a: ASP13ASN, GLU64GLN, THR67LEU	GLU64GLN	ASP13GLU
U09b: ASP13ASN and GLU64GLN	THR67LEU	GLU17ASP
		GLU64ASP

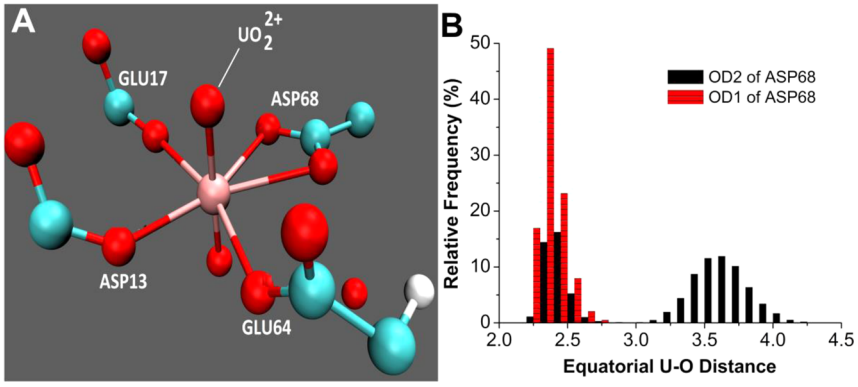

Figure 1. (A) Snapshot of UO_2^{2+} in SUP. (B) Normalized histograms showing the interactions between UO_2^{2+} and the two carboxylate oxygen atoms of ASP68.

atoms) to $\lambda = 0$; XX_2^0 (charge and vdW parameters of dummy atoms, X)]. The equilibration and sampling periods were expanded to 1 and 5.3 ns, respectively, for each window to allow adequate relaxation of the protein upon perturbation of the Hamiltonian by conversion of UO_2^{2+} to XX_2^0. In XX_2^0, the bond and angle parameters were kept the same as those in UO_2^{2+}. To prevent uncontrolled collisions of the dummy atoms of XX_2^0 with other atoms, we carried out simulations in which harmonic potentials of about 1000−2000 kJ/nm^2 were used to maintain the relative positions of the center of mass of UO_2^{2+}/XX_2^0 with that of the protein. The overall effect of this potential on the calculated binding energy of UO_2^{2+} to the proteins was eliminated by assuming a similar effect during UO_2^{2+}/XX_2^0 mutations in a water box (without the protein). This is reasonable given that UO_2^{2+} is located at the surface of the protein, in contact with water. We ascertained that in all cases the XX_2^0 group gradually diffuses into water as it is slowly decoupled away from the protein. As such, when the harmonic potentials are not utilized, the XX_2^0 group behaves as it would in aqueous phase simulations. The error bars associated with the computed free energies were obtained with the block-averaging method. The MD simulations and associated analyses were carried out with GROMACS 4.6.3.[34,35] Further details are given in the Supporting Information.

List of Mutations. The mutants of SUP that were studied in this work are listed in Table 1. Of these proteins, Zhou et al. have experimentally characterized SUP, U09a, and U09b.[13] There are three joint mutations between SUP and U09a. We studied each of these intermediate mutations to determine whether any of them can separately improve UO_2^{2+} capture. The remaining four proteins are potential candidates for improved UO_2^{2+} capture that are identified in the present work by studying the binding pocket of SUP.

DFT Calculations. DFT calculations were performed to elucidate the properties of UO_2^{2+} complexes with the oxygen atoms of carboxylate and water ligands. As the SUP protein is too big to be modeled with DFT calculations, we have replaced the amino acids involved in UO_2^{2+} capture by acetate (CH_3COO^-) groups. This simplification greatly reduces the cost of our calculations and allows for a good description of the first shell around UO_2^{2+}; see the Supporting Information for details. The calculations were performed with the Amsterdam Density Functional (ADF) code.[36] The zeroth order regular approximation (ZORA)[37,38] was used to include scalar relativistic effects. All atoms were described with Slater type orbitals of double-ζ polarized (DZP) quality except for U, Cu, and V which were described with triple-ζ polarized basis sets (TZP). The M06[39,40] functional was used in these calculations. The combination of hybrid or meta-hybrid functionals with high quality basis sets has been used to accurately predict the structural properties and energetics of actinide complexes in solution.[30,41−45] It has also been found that the M06 functional performs accurately for predicting the redox potentials of aqueous actinyl complexes.[46] Aqueous phase calculations were carried out with the conductor screening solvation model (COSMO).[47,48] The vibrational frequencies of the optimized structures were calculated. The coordination of UO_2^{2+} by acetate and other monocarboxylate anions have been examined previously by other workers. This allows us to check the accuracy of our computations with previously reported experimental and theoretical results.[41,49−51]

RESULTS AND DISCUSSION

Coordination Environment of UO_2^{2+} in SUP. *First Coordination Sphere around UO_2^{2+}.* The first coordination sphere of UO_2^{2+} bound to aqueous SUP obtained from MD simulations is shown in Figure 1. The equatorial region is occupied by four amino acid residues that bind UO_2^{2+} through five U−O bonds. These residues are ASP68, GLU17, GLU64, and ASP13. Two of these, GLU64 and ASP13, always bind to UO_2^{2+} in a monodentate fashion. In contrast, ASP68 binds to UO_2^{2+} in a bidentate fashion when GLU17 is bound in a monodentate fashion (Figure 1), and conversely, it binds in a monodentate fashion when GLU17 is coordinated in a bidentate fashion. The average lengths of the bonds between UO_2^{2+} and these amino acids are presented in Table 2.

dx.doi.org/10.1021/ja5087563 | J. Am. Chem. Soc. 2014, 136, 17484−17494

Table 2. Structural Features (Å) of the First Coordination Sphere of UO_2^{2+} in SUP, U09a, and U09b Obtained from MD Simulations in Aqueous Solution[a]

	N_{H_2O}	$U-O_{H_2O}$	N_{AA}	$U-O_{ASP68}$	$U-O_{GLU17}$	$U-O_{GLU64/GLN64}$	$U-O_{ASP13/ASN13}$
SUP	0		5	2.38; 3.17	2.53; 3.02	2.32; 4.13	2.33; 3.89
U09a	2	2.48; 2.49	4	2.46; 2.54	2.40; 2.66		
U09b	2	2.48; 2.49	4	2.43; 2.46	2.51; 2.53		

[a]The number of water ligands, N_{H_2O}, and the number of bonds to coordinated amino acid residues, N_{AA}, are presented. The bonds of UO_2^{2+} to water ($U-O_{H_2O}$) and amino acid residues are also presented.

Table 3. Structural Features (Å) of the First Coordination Sphere of UO_2^{2+} in SUP Obtained from MD Simulations at around pH 4.5[a]

	N_{H_2O}	$U-O_{H_2O}$	N_{AA}	$U-O_{ASP68}$	$U-O_{GLU17}$	$U-O_{GLU64}$	$U-O_{ASP13}$
SUP-(ASP13)	1	2.47	4	2.38; 3.17	2.53; 3.02	2.40; 4.23	
SUP-(GLU64)	1	2.47	4	2.46; 2.54	2.44; 2.46		2.36; 4.06
SUP-(ASP13GLU64)	1	2.47	4	2.48; 2.48	2.46; 2.47		
SUP-(all four)	1	2.47	2−4	2.42; 2.74	2.43; 3.36		
X-ray[13]	1	2.30	2−4	2.69; 2.91	2.36; 3.09		

[a]SUP-(all four) is the case in which the side chains of ASP13, GLU17, GLU64, and ASP68 have all been protonated.

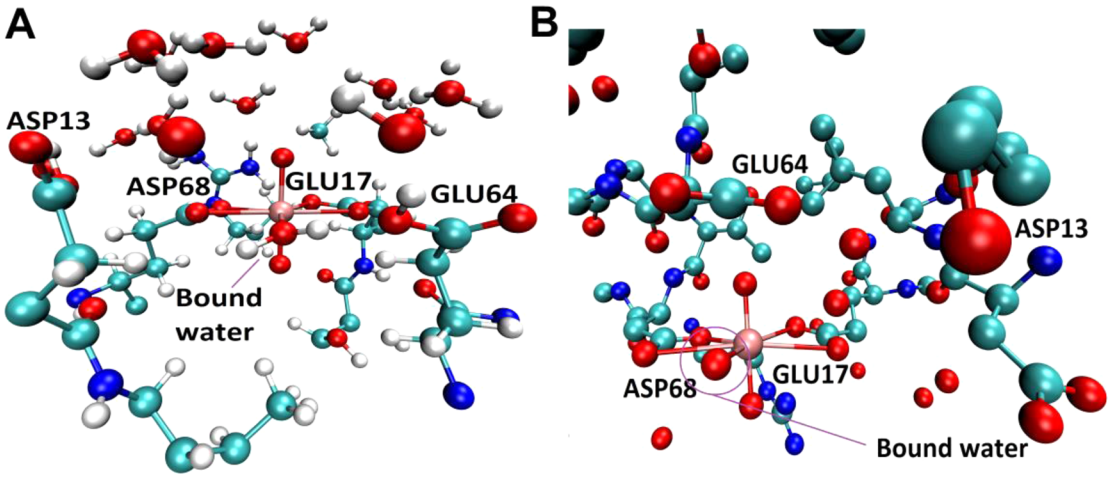

Figure 2. (A) Average snapshot of UO_2^{2+} in SUP obtained from the last 10 ns of 90 s MD simulations carried out after protonating the side chains of the ASP13 and GLU64 residues. The pK_a's of ASP and GLU residues are about 4.4−4.6 in proteins, nearly identical to the pH at which crystal structures were obtained for UO_2^{2+} bound to SUP. (B) The binding site geometry in the experimental crystal structure.

We also carried out simulations that mimic pH 4.5, the conditions at which the crystal structures were obtained. As the expected pK_a values of the side chains of ASP and GLU residues in proteins are around 4.4−4.6,[52] we considered cases in which the side chains of one (ASP13 or GLU64), two (ASP13 and GLU64), or all of the amino acid residues found around UO_2^{2+} were protonated. The side chains of the ASP13 and GLU64 residues are likely to have slightly higher pK_a values than those of ASP68 and GLU17, due to the larger distance between one of their carboxylate oxygen atoms and the highly charged UO_2^{2+} moiety (Table 2). The structural features obtained from these simulations are presented in Table 3. After simulations for 0.5−1.2 ns, the protonated amino acid residue(s) is removed from the first coordination sphere and replaced by a water ligand, a process that was not reversed over simulation times that extended up to 90 ns. When ASP13 or GLU64 is protonated, it exits the first coordination sphere and its acidic OH group forms hydrogen bonds with the carboxylate of GLU64 or ASP68, respectively, bound to UO_2^{2+}, while its C═O group forms hydrogen bonds with a proton of the coordinated water. When ASP13 and GLU64 are both protonated, they both exit the first coordination sphere and stabilize the amino acid residues in the first coordination sphere as well as the water ligand now coordinated to UO_2^{2+} (Figure 2A). When all four amino acid residues are protonated, only the side chain C═O groups of ASP68 and GLU17 remain coordinated to UO_2^{2+}. The structural arrangements of the first coordination sphere in the SUP-(ASP13GLU64) and SUP-(all four) cases agree well with the experimental crystal structures, suggesting that the methodology and force fields used in our simulations are able to reproduce the binding site geometry at various pH values.

Axial Region of Coordination Sphere around UO_2^{2+}. The coordination of UO_2^{2+} to aqueous SUP (pH 7.0) is such that one oxygen atom is embedded in the protein while the other is exposed to the aqueous environment (Figure 3). For the exposed oxygen atom, the protons of the surrounding water are 2.6−5.0 Å apart. In Figure 3, we also show the radial distribution function (RDF) between the exposed oxygen atom and the protons of the surrounding water. This figure is very similar to the RDF obtained for the contacts between the oxygen atoms of UO_2^{2+} and the protons of water in aqueous

dx.doi.org/10.1021/ja5087563 | J. Am. Chem. Soc. 2014, 136, 17484−17494

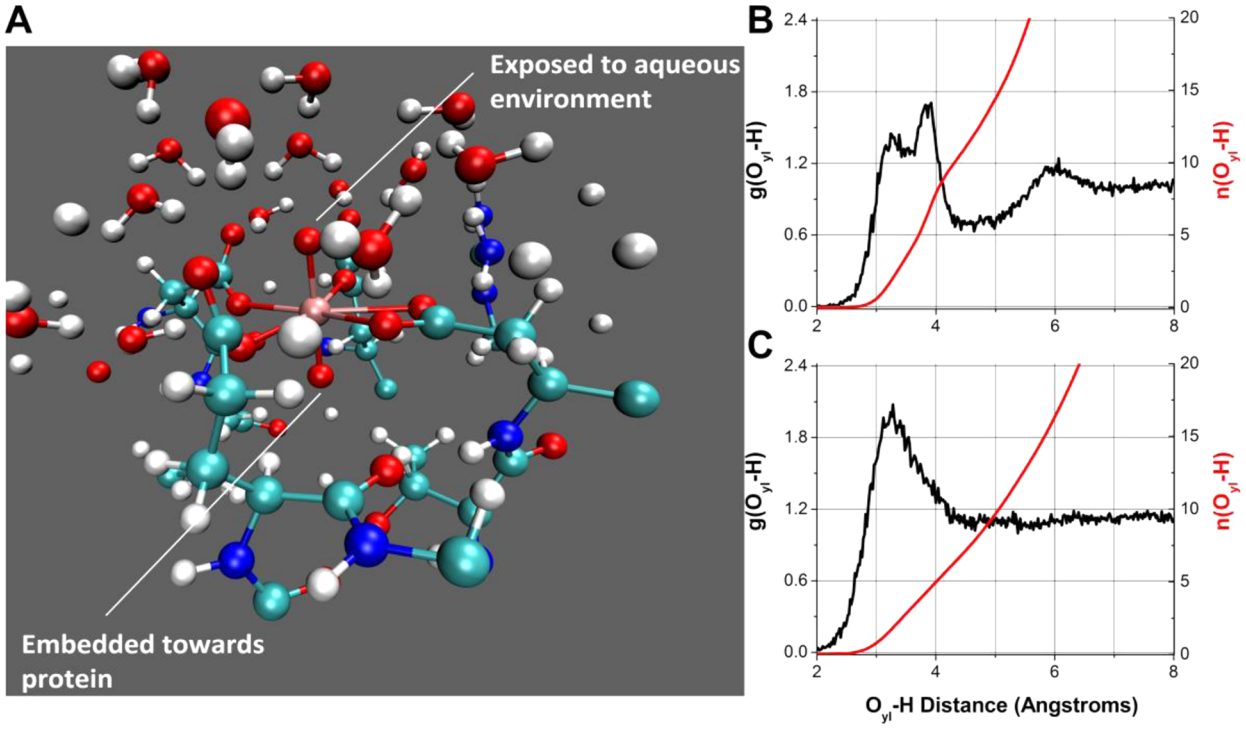

Figure 3. (A) The position of UO_2^{2+} relative to the protein and the surrounding water molecules. The RDF, $g(O_{yl}–H)$, and its integral, $n(O_{yl}–H)$, between the oxygen atoms of UO_2^{2+} and the protons of surrounding water molecules in (B) aqueous UO_2^{2+} and (C) UO_2^{2+} embedded in SUP.

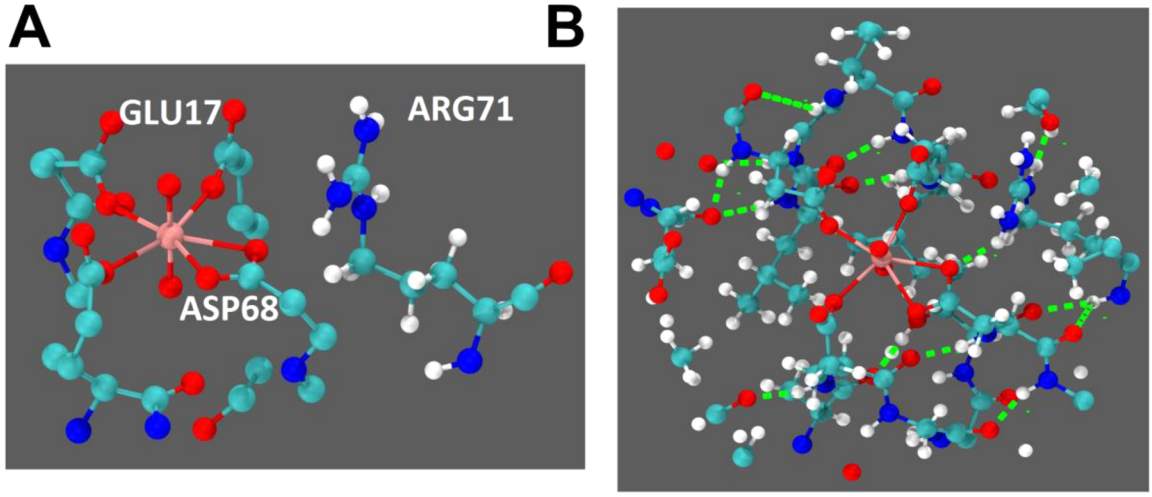

Figure 4. (A) Average positions of the guanidinium protons of ARG71 near the carboxylate oxygen atoms of ASP68 and GLU17. (B) Hydrogen bonds (blue dashed lines) found in the second coordination sphere of UO_2^{2+}.

solution (Figure 3). The protein reduces the space available for water molecules found around the exposed oxygen atom of UO_2^{2+} in SUP. As a result, there are only about 10 water molecules 2.0–5.0 Å apart from the exposed oxygen atom of UO_2^{2+} (Figure 3). Bare UO_2^{2+} in water has instead 15 water molecules in the same distance range (Figure 3). The protein also induces a more structured distribution of the water molecules above the exposed oxygen of UO_2^{2+} in SUP, as illustrated by the presence of only one peak in the RDF obtained in the protein environment (Figure 3).

Second Coordination Sphere around UO_2^{2+}. The carboxylate oxygen atoms of the amino acid residues bound to UO_2^{2+} interact through hydrogen bonds with the amine, guanidinium, or ammonium protons of neighboring residues found in the second coordination sphere (Figure 4). For example, the guanidinium protons of ARG71 form hydrogen bonds with the carboxylate oxygen atoms of ASP68 and GLU17 (Figure 4A). The oxygen atom of UO_2^{2+} exposed to the water environment (Figure 3) interacts only weakly (average distance of 4.0 Å) with the guanidinium protons of ARG71. THR67 is also one of the amino acids found in the second shell around UO_2^{2+}. THR67, like ARG71, interacts with several amino acids through hydrogen bonds. There are many other hydrogen bonds in the second shell around UO_2^{2+} (Table SI1, Supporting Information). The overall effect is that there is an amino acid hydrogen bond network that spans the equatorial region of UO_2^{2+} (Figure 4B). Further details regarding the interaction of

dx.doi.org/10.1021/ja5087563 | J. Am. Chem. Soc. 2014, 136, 17484–17494

Table 4. Scaled Binding Free Energies (kJ/mol) of UO_2^{2+} to Several Proteins[a]

	simulations		expt.		simulations	
proteins	free energy	k_1/k_2	k_1/k_2	intermediate proteins	free energy	k_1/k_2
SUP	−196.1 ± 5.3	1.0	1.0	ASP13ASN	−143.8 ± 6.4	1.3×10^9
U09a	−116.1 ± 1.6	8.5×10^{13}	5.0×10^6	GLU64GLN	−133.3 ± 13.9	8.6×10^{10}
U09b	−130.0 ± 2.2	3.2×10^{11}	2.4×10^5	THR67LEU	−166.9 ± 2.2	1.2×10^5

	simulations	
potential proteins	free energy	k_1/k_2
ASP68GLU	−178.2 ± 4.2	1.3×10^3
ASP13GLU	−180.8 ± 6.4	4.6×10^2
GLU17ASP	−174.1 ± 4.9	6.8×10^3
GLU64ASP	−213.5 ± 9.9	9.3×10^{-4}

[a]The binding free energies of UO_2^{2+} to these proteins have been scaled with the calculated binding free energy (1402 ± 6.7 kJ/mol) of UO_2^{2+} to water. k_1/k_2 is the ratio between the calculated equilibrium constants of UO_2^{2+} capture by SUP to that of other proteins.

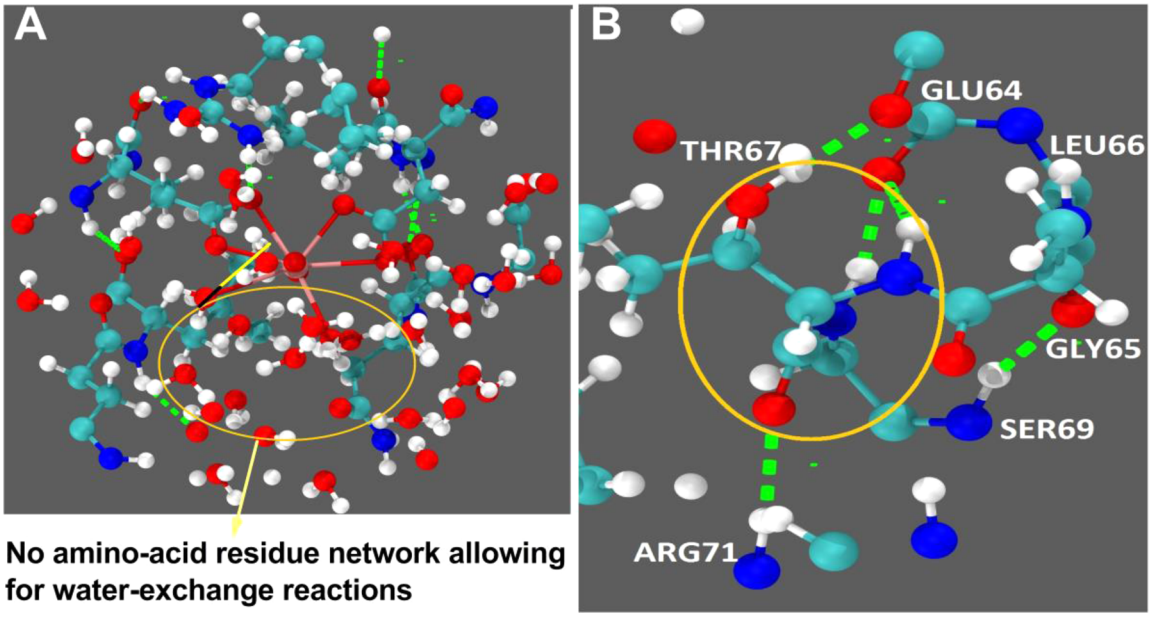

Figure 5. (A) The coordination environment of UO_2^{2+} in U09a. There is a gap in the hydrogen bond network between amino acids in the second coordination sphere. (B) Hydrogen bond interactions of THR67 with neighboring amino acids.

UO_2^{2+} with the protein are given in Figures SI1−5 of the Supporting Information.

Effects of Mutations on Sensitivity for UO_2^{2+}. Zhou et al.[13] prepared some proteins with much lower sensitivities for UO_2^{2+} than SUP. These proteins are all mutants of SUP. Two of these proteins are U09a and U09b. U09a has ASN13, GLN64, and LEU67 residues instead of ASP13, GLU64, and THR67 in SUP (Table 1). U09b has ASN13 and GLN64 instead of ASP13 and GLU64 found in SUP. The probability of UO_2^{2+} dissociating from these proteins at equilibrium is expressed as the dissociation constant. The experimental dissociation constants of UO_2^{2+} from SUP, U09b, and U09a are 7.4 fM, 1.8 nM, and 37 nM, respectively.[13] The mutations found in U09a and U09b significantly affect the UO_2^{2+} capture ability of the protein. To understand how these mutations influence UO_2^{2+} capture, we calculated the binding free energies of UO_2^{2+} to SUP, U09a, and U09b. The results are reported in Table 4. In Table 4, the overall binding energies of UO_2^{2+} to the proteins are scaled with the binding free energy of UO_2^{2+} to water to form $[UO_2(H_2O)_5]^{2+}$. We note that Soderholm et al.[53] have experimentally demonstrated that the energy difference between $[UO_2(H_2O)_5]^{2+}$ and $[UO_2(H_2O)_4]^{2+}$ is very small, in agreement with theoretical predictions.[28,54]

The binding free energy of UO_2^{2+} to SUP was calculated as −196.1 ± 5.3 kJ/mol. This value has a negative sign, meaning that UO_2^{2+} capture by SUP is spontaneous. In addition, it is larger than those of −130.0 ± 2.2 and −116.1 ± 1.6 kJ/mol obtained for U09b and U09a, respectively (Table 4). This means that SUP binds UO_2^{2+} more strongly than U09a and U09b, in agreement with experiments.[13] Methodologically, the ratios of the equilibrium constant of UO_2^{2+} capture by SUP to that of UO_2^{2+} capture by U09a and U09b, depicted as k_1/k_2, are overestimated by the MD simulations by about 10^6−10^7. This is not surprising and corresponds to a maximum error of about 28−41 kJ/mol in the calculated differences in the binding free energies of the proteins. Quantitatively, the trend in the affinities of SUP, U09a, and U09b for UO_2^{2+} is however clear from the MD simulations and agrees with the experiment.

The lower affinity of U09a for UO_2^{2+} is explained *qualitatively* by the fact that it is coordinated only to GLU17 and ASP68 in U09a. The captured UO_2^{2+} is not bonded to ASN13 and GLN64 (Table 2). As a result, the capture of UO_2^{2+} by U09a can be represented by reaction 1 in contrast to

dx.doi.org/10.1021/ja5087563 | J. Am. Chem. Soc. 2014, 136, 17484−17494

reaction 2 for SUP. In these *illustrative* reactions that were inspired by the results of our MD simulations, the amino acids involved in binding UO_2^{2+} are represented simply as "AA". Coordination of a dication to four negatively charged amino acids would be expected to be more exoergic than coordination to two amino acids. Electrostatic considerations therefore dictate that SUP will bind UO_2^{2+} more effectively than U09a.

$$\text{U09a: } [UO_2(H_2O)_5]^{2+} + 2AA^- \rightarrow [UO_2(AA)_2(H_2O)_2] + 3H_2O \quad (1)$$

$$\text{SUP: } [UO_2(H_2O)_5]^{2+} + 4AA^- \rightarrow [UO_2(AA)_4]^{2-} + 5H_2O \quad (2)$$

The first coordination sphere of UO_2^{2+} in U09a also includes two water ligands (Table 2), as the side-by-side coordination of GLU17 and ASP68 to UO_2^{2+} allows for the coordination of two water ligands (Figure SI5, Supporting Information). In U09a, the hydrogen bond network around UO_2^{2+} in SUP (Figure 4B) has been disrupted and does not surround the equatorial region (Figure 5A). The water ligands coordinated to UO_2^{2+} form hydrogen bonds with water molecules in the second coordination sphere as well as with some amino acid residues. These interactions are however weaker than the hydrogen-bond network in SUP (Figure 4B). For this reason, the two water ligands coordinated to UO_2^{2+} can be exchanged with surrounding water. The influence of outer-shell residues on the number of metal-bound carboxylates in metalloproteins has been previously discussed.[55] Overall, however, the capture of UO_2^{2+} by U09a is associated with a loss of translational entropy contribution to the binding free energy. This is because only three water ligands were released in U09a during UO_2^{2+} capture, compared to all five in SUP. This reduction in the translational entropic contribution to the binding free energy relates to the difference between the translational entropy of positionally ordered water ligands bound to UO_2^{2+} and the entropy of bulk water.[56−58] In summary, U09a is less sensitive than SUP, as it binds UO_2^{2+} more weakly, coordinates to UO_2^{2+} only through two amino acid residues, and loses translational entropy, as not all bound water ligands in the first coordination sphere were replaced by amino acids during the capture of UO_2^{2+}.

The coordination environment of UO_2^{2+} in U09b is similar to that of U09a. However, the LEU67THR mutation that converts U09a to U09b results in shorter bonds between the UO_2^{2+} and the amino acids found in the first shell. The equatorial U—O bonds to the amino acid residues are on average slightly shorter in U09b (2.48 Å) than in U09a (2.52 Å) (Table 2). In addition, the side chain of THR67 in U09b is $CH(OH)CH_3$, while that of LEU67 in U09a is $CH_2CH(CH_3)_2$. The side chain OH of THR67 interacts with GLU64, while its amide C═O and N—H groups interact with the guanidinium protons of ARG71 and the amide C═O group of ALA63, respectively (Figure 5B). These interactions are missing in U09a. THR67 therefore provides less steric repulsion to the protein backbone than LEU67, allowing for better coordination between GLU17 and UO_2^{2+} (Table 2). In summary, the combination of slightly shorter U—O bonds in U09b and greater hydrogen bonding in the second coordination sphere are supportive of the trends in the calculated binding free energies (Table 4), as well as with the experimental determination of the dissociation constants of U09a as 37 nM, far larger than that of U09b, 1.8 nM.[13]

Origins of UO_2^{2+} Selectivity in SUP. As previously noted, SUP is very selective for UO_2^{2+}, with Cu^{2+} and VO^{2+} being 3400−9400 times less competitive and other cations (such as Ca^{2+}, K^+, and Mg^{2+}) being 10^5−10^8 times less competitive.[13] We calculated the differences between the binding free energies of UO_2^{2+} and Ca^{2+} (as well as Cu^{2+}, Mg^{2+}, and Zn^{2+}) to SUP as well as those of UO_2^{2+} and Ca^{2+} to several SUP mutants.

For SUP, UO_2^{2+} is more tightly bound than Ca^{2+}. The equatorial bonds between UO_2^{2+} and the first-shell amino acids of SUP are 2.32−2.53 Å long (Table 2). In contrast, for Ca^{2+} coordinated to SUP, the bonds to the amino acid residues are much longer, 2.52−2.79 Å. We show the average coordination environment of Ca^{2+} coordinated to SUP in Figure 6.

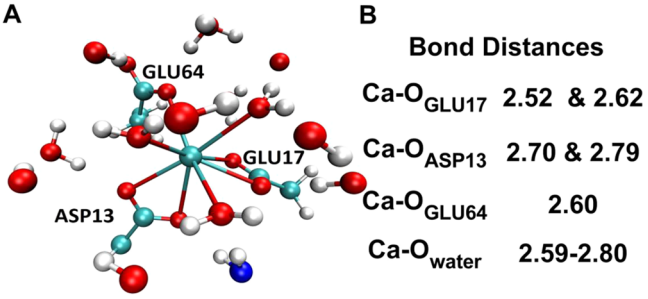

Figure 6. (A) Snapshot of the coordination environment of Ca^{2+} bound to SUP. The amino acid residues have been truncated. (B) Average bond distances (Å) between Ca^{2+} and the first-shell amino acid residues or water ligands. The $Ca-O_{water}$ distances are somewhat larger than those found in aqueous solutions (i.e., without SUP).

Additionally, in SUP, UO_2^{2+} is bound by five oxygen atoms from four amino acids (ASP13, GLU17, GLU64, and ASP68), while Ca^{2+} is coordinated to five oxygen atoms from only three amino acids (ASP13, GLU17, and GLU64) as well as to three water ligands. In all simulations, Ca^{2+} is never coordinated to ASP68. Therefore, Ca^{2+} bound to aqueous SUP has a coordination number of about eight. This coordination number is not unusual, as several studies have shown that Ca^{2+} has a coordination number of about eight in water.[59−62] Overall, the coordination of Ca^{2+} by SUP can be represented by reaction 3. This reaction is analogous to reactions 1 and 2 where the amino acid residues coordinated to the

$$[Ca(H_2O)_8]^{2+} + 3AA^- \rightarrow [Ca(AA)_3(H_2O)_3]^- + 5H_2O \quad (3)$$

metal ion are represented as "AA". Electrostatic considerations suggest that reaction 2 (UO_2^{2+} coordination to SUP) would be more exoergic than **3**. The presence of three water molecules in the first coordination sphere around Ca^{2+} is also disadvantageous, as the full entropic contribution to the binding free energy (if all eight water ligands were replaced) is not realized. The differences between the binding free energies of UO_2^{2+} and Ca^{2+} to SUP are presented in Table 5.

In Table 5, the differences between the binding free energies of UO_2^{2+} and Ca^{2+} to SUP, U09a, and U09b are all positive, indicating that these proteins preferentially complex UO_2^{2+} rather than Ca^{2+}. The value obtained for SUP (42.3 ± 4.9 kJ/mol) is however much higher than those of U09a and U09b (27.3 ± 8.3 and 37.5 ± 10.1 kJ/mol, respectively), indicating that these proteins are not as selective for UO_2^{2+} as SUP and that they bind UO_2^{2+} less effectively than SUP.

dx.doi.org/10.1021/ja5087563 | J. Am. Chem. Soc. 2014, 136, 17484−17494

Table 5. Calculated Differences between the Binding Free Energies (kJ/mol) of UO_2^{2+} and Several Ions to Some Proteins[a]

	simulations		expt.[13]		simulations	
proteins	free energy[b]	k_1/k_2[c]	k_1/k_2[c]	intermediate proteins	free energy[b]	k_1/k_2[c]
SUP	42.3 ± 4.9	2.3×10^7	1.9×10^6	ASP13ASN	40.8 ± 6.6	1.3×10^7
SUP-Mg^{2+}	44.5 ± 5.2	5.6×10^7	3.4×10^6	GLU64GLN	46.2 ± 3.2	1.1×10^8
SUP-Zn^{2+}	39.8 ± 3.8	8.5×10^6	2.0×10^6	THR67LEU	29.5 ± 1.3	1.4×10^5
SUP-Cu^{2+}	28.0 ± 1.6	7.5×10^4	3.4×10^3			
U09a	27.3 ± 8.3	5.7×10^4				
U09b	37.5 ± 10.1	3.4×10^6				

	simulations	
potential proteins	free energy[b]	k_1/k_2[c]
ASP68GLU	43.1 ± 6.1	3.2×10^7
ASP13GLU	46.2 ± 3.3	1.1×10^8
GLU17ASP	39.7 ± 4.9	8.2×10^6
GLU64ASP	50.2 ± 4.7	5.5×10^8

[a]The values presented in this table are for the UO_2^{2+}–Ca^{2+} pair except where indicated. [b]These energy differences are given relative to the calculated difference between the hydration energies of UO_2^{2+} and the M^{2+} ions (calculated as 117.5, −424.3, −454.9, and −408.0 kJ/mol for the UO_2^{2+}/Ca^{2+}, UO_2^{2+}/Cu^{2+}, UO_2^{2+}/Zn^{2+}, and UO_2^{2+}/Mg^{2+} pairs, respectively; these are comparable with experimental[63−67] values of 41.0, −464.0, −409.2, and −284.1 kJ/mol, respectively). [c]k_1/k_2 are the calculated equilibrium constants of UO_2^{2+}–M^{2+} (where M = Ca, Cu, Mg, or Zn) conversion in SUP or UO_2^{2+}–Ca^{2+} conversion in other proteins. They denote the degree of selectivity of the proteins for UO_2^{2+} over the M^{2+} ions.

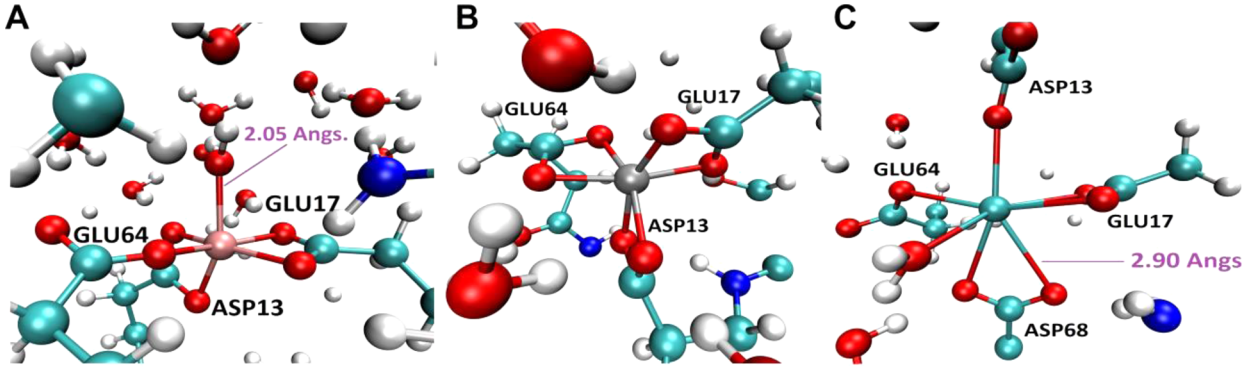

Figure 7. Average snapshots of the coordination environments of (A) Mg^{2+}, (B) Zn^{2+}, and (C) Cu^{2+} bound to SUP. The amino acid residues have been truncated.

Mg^{2+} is bound to aqueous SUP in a similar fashion as Ca^{2+}, with the exception that this ion has only one water ligand in its first coordination sphere in contrast to three for Ca^{2+} (Figure 7). As a result, Mg^{2+} has a coordination number of six when it is bound to aqueous SUP, in agreement with recent studies[59,61] that have found that it has a coordination number of six in aqueous solution. Complexation of Mg^{2+} to SUP can be written as reaction 4, which can also be expected to be less exoergic than reaction 2 based on electrostatic considerations. In contrast to Mg^{2+}, Zn^{2+} is bound to three amino acid residues of SUP through six oxygen atoms, with no water ligand found in its first coordination sphere during 90 ns of simulations (Figure 7). This suggests entropic effects due to water exchange between the first coordination sphere around the metal ion and the disordered water environment would be absent for Zn^{2+}.

$$[Mg(H_2O)_6]^{2+} + 3AA^- \rightarrow [Mg(AA)_3(H_2O)]^- + 5H_2O \quad (4)$$

In contrast to Ca^{2+}, Mg^{2+}, and Zn^{2+} which are coordinated to only three residues, Cu^{2+} is coordinated to four amino acids through five Cu–O bonds (Figure 7) as well as a water ligand (average Cu–O length of 2.55 Å). The carboxylate oxygen atom of ASP68 involved in binding Cu^{2+} can be exchanged, with the overall effect that the Cu–O bond to this residue is on average about 2.75 Å long, slightly longer than the bonds to the other amino acid residues in the first coordination sphere (~2.52 Å). The overall coordination number of Cu^{2+} bound by SUP is six, and the overall complexation reaction can be written as reaction 5, which can reasonably be expected to be more exoergic than reactions 3 and 4 as well as Zn^{2+} capture by SUP.

$$[Cu(H_2O)_6]^{2+} + 4AA^- \rightarrow [Cu(AA)_4(H_2O)]^- + H_2O \quad (5)$$

Although examination of Figure 7 as well as reactions 2, 3, 4, and 5 provides a qualitative trend of $UO_2^{2+} > Cu^{2+} > (Mg^{2+} \sim Zn^{2+} \sim Ca^{2+})$, already in good agreement with the experimental trend,[13] a more quantitative perspective can be obtained by examining the free energy differences presented in Table 5. The overall trend obtained from the free energy MD simulations, $UO_2^{2+} > Cu^{2+} > Zn^{2+} \sim Ca^{2+} > Mg^{2+}$, is in fairly good agreement with experimental data, even though the calculated k_1/k_2 overestimate the experiment (Table 5). The conversion of UO_2^{2+} to Cu^{2+} is less endoergic than the conversion of UO_2^{2+} to any of Mg^{2+}, Zn^{2+}, or Ca^{2+}, as expected from the coordination chemistry of the binding site (Figure 7), illustrating the prominent roles of the binding site geometry and coordination motif on the sensitivity and selectivity of SUP for a metal ion.[13] It is likely that UO_2^{2+}, Cu^{2+}, and VO^{2+} form a

dx.doi.org/10.1021/ja5087563 | J. Am. Chem. Soc. 2014, 136, 17484−17494

Table 6. Structural Features (Å) of the First Shell around UO_2^{2+} in Some Mutant Proteins

	N_{H_2O}	U−O_{H_2O}	N_{AA}	U−O_{ASP68}	U−O_{GLU17}	U−$O_{GLU64/GLN64}$	U−$O_{ASP13/ASN13}$
ASP68GLU	1	2.44	3		2.32; 3.86	2.32; 4.06	2.33; 4.40
ASP13GLU	0		5	2.46; 2.46	2.31; 4.03	2.32; 4.29	2.31; 4.19
GLU17ASP	1	2.44	4	2.39; 2.44	2.31; 4.22	2.31; 3.98	
GLU64ASP	0		5	2.38; 3.22	2.35; 3.13	2.32; 4.15	2.35; 3.80

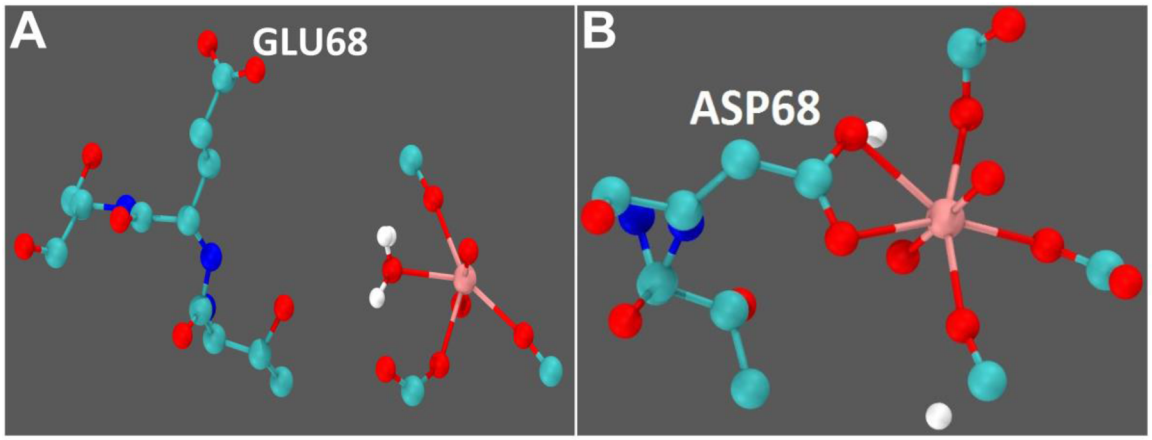

Figure 8. (A) GLU68 residue in the ASP68GLU mutant. (B) ASP68 residue in SUP.

class of ions that bind to four amino acid residues while Mg^{2+}, Zn^{2+}, and Ca^{2+} as well as the other ions examined by Zhou et al.[13] form a class of ions that bind to three (and possibly less) amino acid residues. In support, DFT calculations show that the metal centers of the aqueous complexes of UO_2^{2+} ($UO_2(H_2O)_5^{2+}$ or $UO_2(H_2O)_6^{2+}$) have greater Hirshfeld charges[68] than those of Cu^{2+} ($Cu(H_2O)_4^{2+}$, $Cu(H_2O)_5^{2+}$, or $Cu(H_2O)_6^{2+}$). As a result, UO_2^{2+} forms stronger complexes with the acetate anion than Cu^{2+}.

Search for Protein(s) with Higher UO_2^{2+} Binding Affinities. Comparison of SUP to U09a/U09b has shown that the former provides a better binding configuration for UO_2^{2+} than the latter. This is supported by the calculated binding free energies and follows the experimentally observed trend in the dissociation constants of these proteins.[13] For this reason, we undertook a computational search for proteins more sensitive and selective for UO_2^{2+} using SUP as the template. We used three approaches:

Proteins Intermediate between SUP and U09a/U09b. As noted previously, SUP differs from U09a through three mutations: ASP13ASN, GLU64GLN, and THR67LEU. We examined the influence of these mutations on UO_2^{2+} capture separately. Table 4 shows that the binding free energies of UO_2^{2+} to the ASP13ASN, GLU64GLN, and THR67LEU mutants are between those of SUP and U09a. As these mutants do not bind UO_2^{2+} as effectively as SUP (Table 4), they are also less selective over Ca^{2+} (Table 5). Thus, these mutants are not superior to SUP.

Conversion of ASP68 and ASP13 to GLU. On the basis of the previous results, it seems possible that replacement of the ASP residues in the UO_2^{2+} binding pocket with GLU would result in better binding, because the carboxylate oxygen atoms of GLU are slightly more electronegative than those of ASP residues.[17] For this reason, we studied the ASP68GLU and ASP13GLU mutants. It was found that these mutants do not bind UO_2^{2+} as effectively as SUP (Table 4) and as a result are not as selective for UO_2^{2+} over Ca^{2+} (Table 5). The structural features of the UO_2^{2+} binding pocket in ASP68GLU and ASP13GLU are presented in Table 6. For ASP68GLU, there is no interaction between UO_2^{2+} and the GLU68 residue. This residue is simply too long to fit into the UO_2^{2+} binding pocket. The overall effect is that there are now two water ligands coordinated to UO_2^{2+} (Figure 8). For ASP13GLU, the UO_2^{2+} binding pocket is similar to that found in SUP. As such, its binding free energy to UO_2^{2+} is only slightly lower than that of SUP (Table 4).

Conversion of GLU64 and GLU17 to ASP. After discovering that the GLU68 residue in ASP68GLU precludes coordination with UO_2^{2+} (Figure 8), we decided to study the GLU17ASP and GLU64ASP mutants. In these mutants, we replace GLU residues in the binding pocket with ASP. The ASP and GLU amino acid residues have CH_2COOH and CH_2CH_2COOH side chains, respectively. We hypothesized that the shorter side chain in ASP will allow UO_2^{2+} to bind more strongly with other amino acids in the binding pocket. GLU17ASP binds UO_2^{2+} less strongly than SUP (Tables 4 and 6), because UO_2^{2+} is only coordinated to three amino acid residues through four equatorial bonds, as there are no bonds between UO_2^{2+} and ASP13. There is also one water ligand in the binding pocket. This is different from the coordination mode (five equatorial bonds from four amino acids) found in SUP. These structural properties translate into weaker binding of UO_2^{2+} (Table 4) and poorer selectivity for UO_2^{2+} over Ca^{2+} (Table 5).

On the contrary, in GLU64ASP, UO_2^{2+} is coordinated to four amino acids through five U−O bonds (Table 6). This is similar to the situation found in SUP (Table 2). The ASP64 residue in this mutant reduces the size of the binding pocket with the overall effect that GLU17 has a shorter bond (2.35 Å) to UO_2^{2+} (Table 5) than the distance (2.53 Å) between UO_2^{2+} and GLU17 in SUP (Table 2). The binding free energy of UO_2^{2+} to GLU64ASP was calculated as -213.5 ± 9.9 kJ/mol. This is higher than the value of -196.1 ± 5.3 kJ/mol obtained for SUP (Table 4). Although a difference of about 17.4 ± 15.2 kJ/mol between the binding free energies of UO_2^{2+} by

dx.doi.org/10.1021/ja5087563 | J. Am. Chem. Soc. 2014, 136, 17484−17494

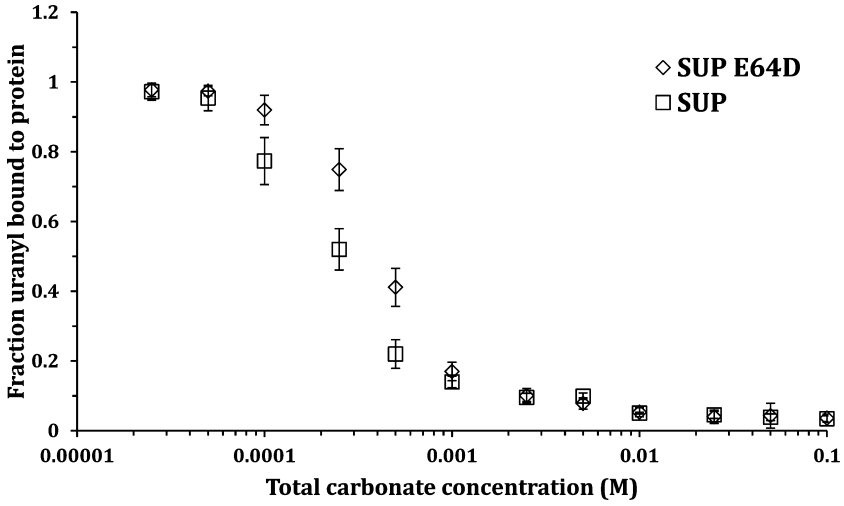

Figure 9. Relative affinities of SUP and its GLU64ASP mutant for UO_2^{2+}. Both curves show a competition assay of protein versus total carbonate for UO_2^{2+}. The experiments were repeated in triplicates, with error bars showing the standard deviation.

GLU64ASP and SUP would appear to be significant, it is important to note that comparison of our simulations to the empirical data for UO_2^{2+} capture by SUP, U09a, and U09b suggested a maximum error of 28−41 kJ/mol. For this reason, we examined the effects of larger sampling times (15 ns rather than the usual 5.3 ns) at each value of λ during the free-energy simulations as well as statistical fluctuations in the free-energy MD runs. For the longer sampling runs, we obtained a difference of 18.1 ± 15.6 kJ/mol between GLU64ASP and SUP. In addition, after five independent free-energy MD runs, we obtained an average difference of 18.3 ± 14.2 kJ/mol between these proteins, confirming that GLU64ASP indeed binds UO_2^{2+} more strongly than SUP.

As GLU64ASP binds UO_2^{2+} more effectively, it is also more selective for UO_2^{2+} over Ca^{2+} (50.2 ± 4.7 kJ/mol) than SUP (42.3 ± 4.9 kJ/mol) (Table 5). Further details of the coordination environment of UO_2^{2+} in GLU64ASP are given in Figure SI7 of the Supporting Information.

Experimental Confirmation. In order to confirm our computational predictions, we performed the GLU64ASP mutation to the previously described SUP protein. The subsequent mutant protein was expressed and purified. Its affinity for UO_2^{2+} was measured using the method previously described.[13] Comparison of the relative affinity of that of SUP and the GLU64ASP mutant showed a modest increase (about 45%) in the binding affinity of the mutant protein (Figure 9). This is consistent with the results of our simulations. This experimental confirmation of our computational approaches and specifically the results in Table 4 give us confidence in our description of the UO_2^{2+} capture properties of SUP and its mutants. Further details of the experimental procedures are given in the Supporting Information.

CONCLUSIONS

The uptake of UO_2^{2+} from aqueous solution by the recently discovered SUP protein and 10 of its mutants has been studied using molecular dynamics and free-energy simulations. On the basis of the results of our simulations, we propose a mutant protein which binds UO_2^{2+} more strongly and that is also more selective for UO_2^{2+} than SUP. To our knowledge, this is the first application of MD and free-energy simulations to understand and improve uranyl−protein interactions.

In SUP, the strong binding of UO_2^{2+} was found to be due to interaction of residues in the first shell and the integrity of the hydrogen bond network in the second shell. Mutant proteins in which the second-shell hydrogen bond network is disrupted have lower UO_2^{2+} binding energies and lower selectivities for UO_2^{2+} over Ca^{2+}. Also, mutants in which the first-shell ASP or GLU residues are replaced by water ligands, ASN or GLN residues have dramatically lower UO_2^{2+} binding energies and lower selectivities for UO_2^{2+} over Ca^{2+}. The selectivity of SUP for a particular metal ion depends crucially on its binding site geometry and coordination environment after it is bound to the protein. We showed that SUP is more selective for ions (like UO_2^{2+} and Cu^{2+}) that bind to four amino acids in the binding site than those that bind to only three amino acid residues.

As a result of a molecular-level understanding of the roles of the first and second shells around UO_2^{2+} on its binding to SUP, we have been able to discover a mutant protein, GLU64ASP, that is more sensitive and selective for UO_2^{2+}. This protein was expressed, and its greater sensitivity for UO_2^{2+} is confirmed experimentally.

ASSOCIATED CONTENT

Supporting Information

Experimental details. Details of computational simulations. Details of computational results. Description of the SUP protein (no bound metal ion). Optimized structures and total energies (in Hartrees) of various complexes. This material is available free of charge via the Internet at http://pubs.acs.org.

AUTHOR INFORMATION

Corresponding Authors

sodoh@umn.edu
gagliard@umn.edu

Notes

The authors declare no competing financial interest.

ACKNOWLEDGMENTS

This work was funded by the Office of Basic Energy Sciences of the U.S. Department of Energy under Grant Numbers ER16087 (S.O.O., G.B., L.G.) and ER15865 (J.K., C.H.). We acknowledge the Minnesota Supercomputing Institute for computing times. R.S. thanks ANR 2010 JCJC 080701

ACLASOLV (Actinoids and Lanthanoids Solvation) for grant support.

REFERENCES

(1) *The Chemistry of the Actinide and Transactinide Elements*, 3rd ed.; Clark, D. L., Hecker, S. S., Jarvinen, G. D., Neu, M. P., Eds.; Springer: Dordrecht, The Netherlands, 2006; Vol. *2.10*, p 815.
(2) Runde, W. Los Alamos Science n. 26 2000 http://fas.org/sgp/othergov/doe/lanl/pubs/00818040.pdf.
(3) Le Clainche, L.; Vita, C. *Environ. Chem. Lett.* **2006**, *4*, 45.
(4) Lee, J. H.; Wang, Z. D.; Liu, J. W.; Lu, Y. *J. Am. Chem. Soc.* **2008**, *130*, 14217.
(5) Pible, O.; Guilbaud, P.; Pellequer, J. L.; Vidaud, C.; Quemeneur, E. *Biochimie* **2006**, *88*, 1631.
(6) Sun, M. H.; Liu, S. Q.; Du, K. J.; Nie, C. M.; Lin, Y. W. *Spectrochim. Acta, Part A* **2014**, *118*, 130.
(7) Van Horn, J. D.; Huang, H. *Coord. Chem. Rev.* **2006**, *250*, 765.
(8) Vidaud, C.; Gourion-Arsiquaud, S.; Rollin-Genetet, F.; Torne-Celer, C.; Plantevin, S.; Pible, O.; Berthomieu, C.; Quemeneur, E. *Biochemistry* **2007**, *46*, 2215.
(9) Wegner, S. V.; Boyaci, H.; Chen, H.; Jensen, M. P.; He, C. *Angew. Chem., Int. Ed.* **2009**, *48*, 2339.
(10) Barkleit, A.; Moll, H.; Bernhard, G. *Dalton Trans.* **2008**, 2879.
(11) Lins, R. D.; Vorpagel, E. R.; Guglielmi, M.; Straatsma, T. P. *Biomacromolecules* **2008**, *9*, 29.
(12) Macaskie, L. E.; Bonthrone, K. M.; Yong, P.; Goddard, D. T. *Microbiology* **2000**, *146*, 1855.
(13) Zhou, L.; Bosscher, M.; Zhang, C. S.; Ozcubukcu, S.; Zhang, L.; Zhang, W.; Li, C. J.; Liu, J. Z.; Jensen, M. P.; Lai, L. H.; He, C. *Nat. Chem.* **2014**, *6*, 236.
(14) http://www.rcsb.org/pdb/explore/explore.do?structureId=4FZO.
(15) http://www.rcsb.org/pdb/explore/explore.do?structureId=4FZP.
(16) http://www.rcsb.org/pdb/explore.do?structureId=2pmr; Vol. *2014*.
(17) Lindorff-Larsen, K.; Piana, S.; Palmo, K.; Maragakis, P.; Klepeis, J. L.; Dror, R. O.; Shaw, D. E. *Proteins* **2010**, *78*, 1950.
(18) Berendsen, H. J. C.; Grigera, J. R.; Straatsma, T. P. *J. Phys. Chem.* **1987**, *91*, 6269.
(19) Parrinello, M.; Rahman, A. *J. Appl. Phys.* **1981**, *52*, 7182.
(20) Hess, B.; Bekker, H.; Berendsen, H. J. C.; Fraaije, J. *J. Comput. Chem.* **1997**, *18*, 1463.
(21) Darden, T.; York, D.; Pedersen, L. *J. Chem. Phys.* **1993**, *98*, 10089.
(22) Nose, S. *Mol. Phys.* **1984**, *52*, 255.
(23) Pomogaev, V.; Tiwari, S. P.; Rai, N.; Goff, G. S.; Runde, W.; Schneider, W. F.; Maginn, E. J. *Phys. Chem. Chem. Phys.* **2013**, *15*, 15954.
(24) Holloczki, O. *Inorg. Chem.* **2014**, *53*, 835.
(25) Maerzke, K. A.; Goff, G. S.; Runde, W. H.; Schneider, W. F.; Maginn, E. J. *J. Phys. Chem. B* **2013**, *117*, 10852.
(26) Aberg, M.; Ferri, D.; Glaser, J.; Grenthe, I. *Inorg. Chem.* **1983**, *22*, 3986.
(27) Buhl, M.; Diss, R.; Wipff, G. *J. Am. Chem. Soc.* **2005**, *127*, 13506.
(28) Gutowski, K. E.; Dixon, D. A. *J. Phys. Chem. A* **2006**, *110*, 8840.
(29) Nichols, P.; Bylaska, E. J.; Schenter, G. K.; de Jong, W. *J. Chem. Phys.* **2008**, *128*, No. 124507.
(30) Shamov, G. A.; Schreckenbach, G. *J. Phys. Chem. A* **2005**, *109*, 10961.
(31) Spencer, S.; Gagliardi, L.; Handy, N. C.; Ioannou, A. G.; Skylaris, C. K.; Willetts, A.; Simper, A. M. *J. Phys. Chem. A* **1999**, *103*, 1831.
(32) Kollman, P. *Chem. Rev.* **1993**, *93*, 2395.
(33) Guilbaud, P.; Wipff, G. *J. Mol. Struct.: THEOCHEM* **1996**, *366*, 55.
(34) Hess, B.; Kutzner, C.; van der Spoel, D.; Lindahl, E. *J. Chem. Theory Comput.* **2008**, *4*, 435.
(35) Van der Spoel, D.; Lindahl, E.; Hess, B.; Groenhof, G.; Mark, A. E.; Berendsen, H. J. C. *J. Comput. Chem.* **2005**, *26*, 1701.
(36) te Velde, G.; Bickelhaupt, F. M.; van Gisbergen, S. J. A.; Fonseca Guerra, C.; Baerends, E. J.; Snijders, J. G.; Ziegler, T. *J. Comput. Chem.* **2001**, *22*, 931.
(37) van Lenthe, E. *J. Comput. Chem.* **1999**, *20*, 51.
(38) van Lenthe, E.; Baerends, E. J.; Snijders, J. G. *J. Chem. Phys.* **1993**, *99*, 4597.
(39) Zhao, Y.; Truhlar, D. G. *J. Chem. Phys.* **2006**, *125*, No. 194101.
(40) Zhao, Y.; Truhlar, D. G. *Theor. Chem. Acc.* **2008**, *120*, 215.
(41) de Jong, W. A.; Apra, E.; Windus, T. L.; Nichols, J. A.; Harrison, R. J.; Gutowski, K. E.; Dixon, D. A. *J. Phys. Chem. A* **2005**, *109*, 11568.
(42) Odoh, S. O.; Walker, S. M.; Meier, M.; Stetefeld, J.; Schreckenbach, G. *Inorg. Chem.* **2011**, *50*, 3141.
(43) Real, F.; Vallet, V.; Marian, C.; Wahlgren, U. *J. Chem. Phys.* **2007**, *127*, No. 214302.
(44) Schreckenbach, G.; Shamov, G. A. *Acc. Chem. Res.* **2010**, *43*, 19.
(45) Tecmer, P.; Bast, R.; Ruud, K.; Visscher, L. *J. Phys. Chem. A* **2012**, *116*, 7397.
(46) Austin, J. P.; Burton, N. A.; Hillier, I. H.; Sundararajan, M.; Vincent, M. A. *Phys. Chem. Chem. Phys.* **2009**, *11*, 1143.
(47) Klamt, A.; Schuurmann, G. *J. Chem. Soc., Perkin Trans. 2* **1993**, 799.
(48) Pye, C. C.; Ziegler, T. *Theor. Chem. Acc.* **1999**, *101*, 396.
(49) Lucks, C.; Rossberg, A.; Tsushima, S.; Foerstendorf, H.; Scheinost, A. C.; Bernhard, G. *Inorg. Chem.* **2012**, *51*, 12288.
(50) Schlosser, F.; Kruger, S.; Rosch, N. *Inorg. Chem.* **2006**, *45*, 1480.
(51) Vazquez, J.; Bo, C.; Poblet, J. M.; de Pablo, J.; Bruno, J. *Inorg. Chem.* **2003**, *42*, 6136.
(52) Tooney, N. M. *Biophysical chemistry - part I: The conformation of biological, macromolecules*; W. H. Freeman and Company: San Francisco, CA, 1980.
(53) Soderholm, L.; Skanthakumar, S.; Neuefeind, J. *Anal. Bioanal. Chem.* **2005**, *383*, 48.
(54) Atta-Fynn, R.; Johnson, D. F.; Bylaska, E. J.; Ilton, E. S.; Schenter, G. K.; de Jong, W. A. *Inorg. Chem.* **2012**, *51*, 3016.
(55) Dudev, T.; Lim, C. *Annu. Rev. Biophys.* **2008**, *37*, 97.
(56) Amzel, L. M. *Proteins* **1997**, *28*, 144.
(57) Harano, Y.; Kinoshita, M. *Biophys. J.* **2005**, *89*, 2701.
(58) Siebert, X.; Amzel, L. M. *Proteins* **2004**, *54*, 104.
(59) Brancato, G.; Barone, V. *J. Phys. Chem. B* **2011**, *115*, 12875.
(60) Jalilehvand, F.; Spangberg, D.; Lindqvist-Reis, P.; Hermansson, K.; Persson, I.; Sandstrom, M. *J. Am. Chem. Soc.* **2001**, *123*, 431.
(61) Li, P. F.; Roberts, B. P.; Chakravorty, D. K.; Merz, K. M. *J. Chem. Theory Comput.* **2013**, *9*, 2733.
(62) Mancini, G.; Brancato, G.; Barone, V. *J. Chem. Theory Comput.* **2014**, *10*, 1150.
(63) Gibson, J. K.; Haire, R. G.; Santos, M.; Marcalo, J.; de Matos, A. P. *J. Phys. Chem. A* **2005**, *109*, 2768.
(64) Marcus, Y. *Ion Solvation*; John Wiley and Sons Ltd: Chichester, U.K., 1985.
(65) Marcus, Y. *J. Chem. Soc., Faraday Trans. 1* **1991**, *87*, 2995.
(66) Marcus, Y.; Loewenschuss, A. *J. Chem. Soc., Faraday Trans. 1* **1986**, *82*, 2873.
(67) *Handbook on the Physics and Chemistry of Rare Earths*; Rizkalla, E. N., Choppin, G. R., Eds.; North-Holland: Amsterdam, The Netherlands, 1994; Vol. *18*: Lanthanides/Actinides: Chemistry.
(68) Hirshfeld, F. L. *Theor. Chim. Acta* **1977**, *44*, 129.